

JET Experiments to Assess Finite Larmor Radius Effects on Resonant Ion Energy Distribution during ICRF Heating

A. Salmi¹, P. Beaumont², P. de Vries², L.-G. Eriksson³, C. Gowers², P. Helander²,
M. Laxåback⁴, M.J. Mantsinen¹, J.-M. Noterdaeme^{5,6}, D. Testa⁷
and EFDA JET contributors*

¹*Helsinki University of Technology, Association Euratom-Tekes, Finland*

²*Euratom/UKAEA Fusion Association, Culham Science Centre, Abingdon, United Kingdom*

³*Association EURATOM-CEA, CEA-Cadarache, Saint-Paul-Lez Durance, France*

⁴*Alfvén Laboratory, Association Euratom-VR, Stockholm, Sweden*

⁵*Max-Planck IPP-EURATOM Assoziation, Garching, Germany*

⁶*Gent University, Belgium*

⁷*CRPP, Association Euratom-Confédération Suisse, EFPL, Lausanne, Switzerland*

**see annex of J Pamela et al., Fusion Energy 2002 (Proc. 19th Int. Conf. Lyon, 2002) IAEA, Vienna (2002).*

ABSTRACT This work reports on experimental verification of the importance of finite Larmor radius (FLR) effects on the detailed shape of the resonant ion distribution on JET tokamak during ion cyclotron resonance heating (ICRH). It is seen that not taking the FLR effects into account leads to an incorrect local ion temperature prediction. Ion energy distributions are simulated by fully including FLR effects and good agreement with neutral particle analyser (NPA) measurements has been found.

INTRODUCTION The experiments reported here continue an earlier work [1] where it was found that due to finite Larmor radius effects the wave-particle interaction at certain energies E^* becomes strongly reduced, effectively preventing resonating ions from reaching higher energies. This was an important result because it showed that the FLR effects can influence the distribution function of the resonating ions, and thus they can also play a role for the absorption strength. In practise, these effects are mainly of importance for second or higher harmonic ICRF heating scenarios where E^* is rather small, typically around 1 MeV in JET. One of the principal ICRF heating schemes foreseen for ITER is the second harmonic heating of tritium $\omega \approx 2\omega_{cT}$. It is therefore of interest to assess the significance of FLR effects in a second harmonic heating scheme not only for physics interest but also to see whether it has implications on ITER.

RELEVANT ICRH THEORY It is possible to obtain a rough analytical estimate for the perpendicular (to the magnetic field) ion distribution f_{\perp} by solving a simplified Fokker-Planck equation for test particles as in Ref. 2

$$\frac{\partial f(v_{\perp}, t)}{\partial t} \approx -\frac{1}{v_{\perp}} \frac{\partial}{\partial v_{\perp}} (\alpha v_{\perp} f) + \frac{1}{2v_{\perp}} \frac{\partial^2}{\partial v_{\perp}^2} (\beta v_{\perp} f) + \frac{1}{4v_{\perp}} \frac{\partial}{\partial v_{\perp}} (\gamma f) + \frac{1}{v_{\perp}} \frac{\partial}{\partial v_{\perp}} \left(D_{RF} v_{\perp} \frac{\partial f}{\partial v_{\perp}} \right).$$

where α , β and γ are the Spitzer collision coefficients and D_{RF} is the RF diffusion coefficient. Here $D_{RF} \propto |E_{+} J_{n-1}(k_{\perp} v_{\perp} / \omega_{ci}) + E_{-} J_{n+1}(k_{\perp} v_{\perp} / \omega_{ci})|^2$ is the full RF diffusion coefficient and not expansion as in Ref. 2. Integrating twice yields

$$f(v_{\perp}) \approx f_0 \exp\left(-\int_0^{v_{\perp}} dv_{\perp} \frac{-4\alpha v_{\perp} + 2(\beta v_{\perp})' + \gamma}{2\beta v_{\perp} + 4D_{RF} v_{\perp}}\right).$$

In the integrand, for reasonably high power levels, say, $P_{ICRH} > 0.5$ MW at JET, D_{RF} at high energies is large compared to the other terms for a large range of plasma parameters, except

close to one of its minima. D_{RF} will thus dominate the main features of the distribution. Figure 1 shows an example of the relation between the distribution and D_{RF} . Note that E^* is also a function of electron density through the coupling between the density and k_{\perp} and that the distribution is flat when D_{RF} is large and drops rapidly when D_{RF} is small. This is markedly different from the exponential solution for f_{\perp} with the familiar effective tail temperature $T_{eff} \propto p_{\perp} T_e^{3/2} / n_r n_e$ obtained by approximating D_{RF} with an effective constant value (thus ignoring the finite Larmor radius effects) and using approximate Spitzer coefficients as in Ref. 2. Here p_{\perp} is the power density absorbed by resonant species and n_r is their density, T_e is electron

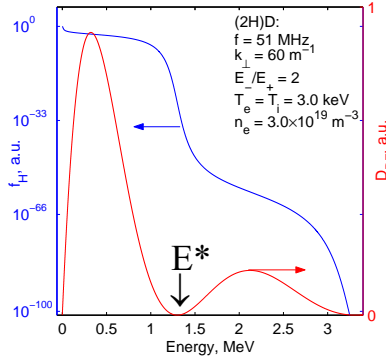
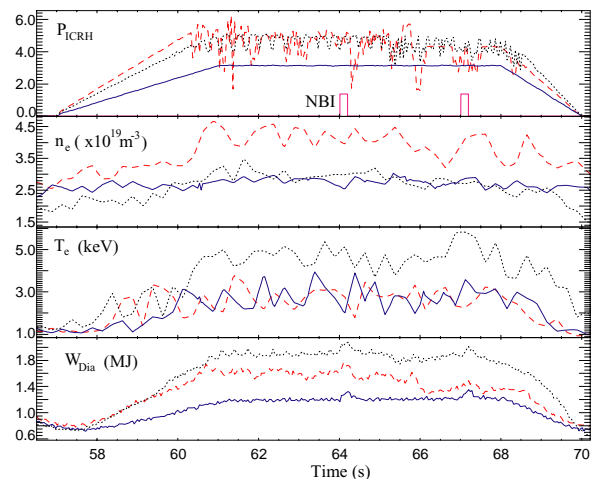


Fig. 1 An illustration of the influence of the RF diffusion coefficient (red curve) on the distribution function (blue curve).

temperature and n_e is electron density.

EXPERIMENT Figure 2 shows ICRH power, neutral beam power (NBI), electron density and temperature at magnetic axis and plasma diamagnetic energy for three discharges 58734, 58738 and 58739. Short duration NBI pulses at 64.1s and at 67.1s were used for diagnosing ion density and

Fig. 2 ICRH and NBI power, (b) central electron density, (c) central electron temperature and (d) plasma diamagnetic energy. Dashed lines (---) correspond to pulse number 58734, full lines (—) to 58738 and dotted lines (•••) to 58739



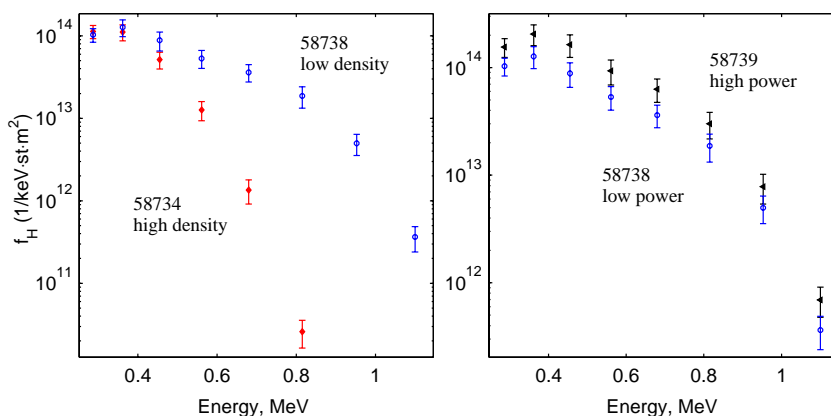
temperature. The discharges are such that both high density pulse 58734 and high power per particle pulse 58739 are to be compared against the reference pulse 58738. Table 1 summarises the most relevant differences and similarities for these comparisons.

Table 1 Key parameters for the discharges. Values are normalised to those of discharge 58738 with an electron density $n_e(0)=2.8 \times 10^{19} \text{ m}^{-3}$, power absorbed by hydrogen $P_H=2.9 \text{ MW}$, electron temperature $T_e(0)=3 \text{ keV}$, hydrogen density $n_H(0)=1.3 \times 10^{18} \text{ m}^{-3}$, ion slowing down time $t_s=0.2 \text{ s}$ and $E^*=1.37 \text{ MeV}$.

Pulse	n_{e0}	P_H	T_{e0}	n_{H0}	T_{eff}	E^*
58734	1,5	1,2	1,0	0,9	0,9	0,7
58738	1,0	1,0	1,0	1,0	1,0	1,0
58739	1,0	1,2	1,7	1,0	2,4	1,0

MEASUREMENTS Line integrated perpendicular energy distribution deduced from NPA [3] measurements for the three pulses (58738 appearing in two plots) are presented in Fig. 3. In the left frame one sees that the energy distribution of the high density (high k_{\perp}) pulse 58734 drops much more rapidly than that of the low density (low k_{\perp}) one 58738. This is

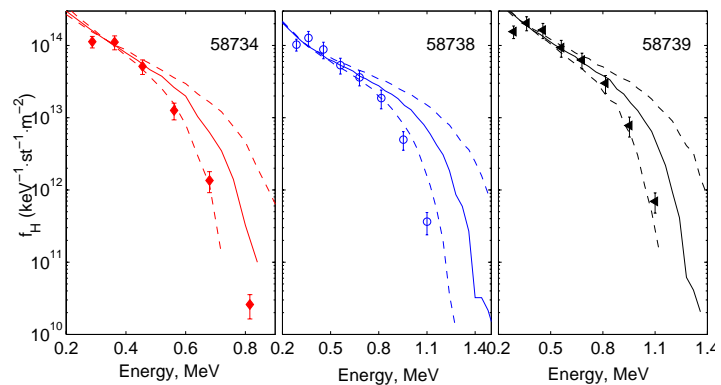
Fig. 3 Experimental hydrogen energy distribution deduced from high-energy NPA measurements with error bars included.



exactly as predicted by theory. Additionally, it shows that local ion temperature for 2nd (or higher) harmonic ICRF heated ions can not be estimated with T_{eff} (see Table 1) giving further evidence for the presence of FLR effects. Moreover, the frame on the right hand side shows a comparison between pulses of equal electron density (equal k_{\perp}). Measured distributions again follow the theory and are similar in shape. T_{eff} , being related to fast ion energy content, sees the difference in energy content but again fails to correctly estimate the local temperature. These complementary comparisons confirm that the resonant particles in the plasma indeed see the details of the RF diffusion operator and are blocked from reaching higher energies due to the weak wave-particle interaction close to energy E^* .

MODELLING Modelling of the resonant particle distribution has been made with a combination of a simplified ICRH power deposition code PION [4] and a 3-D Monte Carlo code FIDO [5] which was used to solve the 3-D Fokker-Planck equation for the distribution function. PION provided the information of the amount of power absorbed by hydrogen and the wave polarisation as well as k_{\perp} -spectrum for FIDO. The energy distributions calculated with this method are presented in Fig. 4 together with the experimental distributions.

Fig. 4 FIDO simulations of proton perpendicular energy distribution (lines) compared with NPA measurements (points with error bars). Dashed (--) lines reflect the uncertainty in modelling due to the uncertainty in electron density.



DISCUSSION Although simulations agree rather well with measurements there are some effects that are not taken into account in simulations but which might have minor effects and are thus discussed briefly. The ratio between sawteeth period and ion slowing down time was roughly equal to unity for each of the discharges. Sawteeth period is considered to be long enough for the distribution to extend into its full length over time and they are thus not considered to be of importance. Electric field amplitude is taken to be constant in FIDO which is not exactly correct and could lead to a small error. Ion adiabatic motion [6] is enhanced when the wave-particle interaction is weak as it is close to E^* . It could augment the suppression of D_{RF} and therefore further reduce the formation of the high energy tail. This was verified with STOCH [7] code for one mode number and one frequency. Although STOCH predicts significant adiabaticity close to E^* it is clear that it would be much reduced when including the whole spectrum and multiple frequencies. Finally, the combination of uncertainties in temperature, ion density as well as parallel and perpendicular wave spectrum can lead to an increased total error.

CONCLUSION The experimental results backed with modelling have shown that FLR effects are responsible for the lack of particles beyond critical energy E^* . This phenomenon gives one an opportunity to tailor the distribution to some extent. Increasing electron density will increase perpendicular wave number and therefore reduce E^* . Reduction of E^* can also be achieved by decreasing magnetic and keeping the resonance position fixed. Due to the stronger magnetic field in ITER and future power plants E^* will typically be higher than it was here. For standard ITER parameters [8] of $n_D = n_T = 5 \cdot 10^{19} \text{ m}^{-3}$, $B_T = 5.7 \text{ T}$, $f = 2f_{cT}$, $k_{\perp} = 52 \text{ m}^{-1}$ and $E_{\perp}/E_{\parallel} = 5$ we get $E^* = 7.5 \text{ MeV}$.

REFERENCES

- [1] M.J. Mantsinen, L-G. Eriksson, A. Gondhalekar, and T. Hellsten, Nuclear Fusion 39 (1999) 459.
- [2] Stix, T.H., Nuclear Fusion 15 (1975) 737
- [3] A.A. Korotkov, A. Gondhalekar, and A.J. Stuart, Nucl. Fusion 37 35 (1997).
- [4] L.-G. Eriksson and T. Hellsten, Phys. Scripta 55 70 (1995).
- [5] J. Carlsson, L.-G. Eriksson and T. Hellsten, Nuclear Fusion 32 (1997) 719.
- [6] Bécoulet, A., Gambier, D. J., Samain, A., Phys. Fluids B 3 (1991) 137.
- [7] Helander, P., Lisak, M., Phys. Fluids B 4 (1992) 1927.
- [8] ITER Physics Expert Group on Energetic Particles et al., Nuclear Fusion 39 (1999) 2495